Physics Letters B 730 (2014) 275–279

Contents lists available at ScienceDirect

Physics Letters B

www.elsevier.com/locate/physletb

Boosting Higgs CP properties via *VH* production at the Large Hadron Collider

Rohini Godbole [a], David J. Miller [b,*], Kirtimaan Mohan [a,c], Chris D. White [b]

[a] *Centre for High Energy Physics, Indian Institute of Science, Bangalore 560 012, India*
[b] *SUPA, School of Physics and Astronomy, University of Glasgow, Glasgow, G12 8QQ, UK*
[c] *LAPTh, Univ. de Savoie, CNRS, B.P. 110, Annecy-le-Vieux, F-74941, France*

ARTICLE INFO

Article history:
Received 26 November 2013
Received in revised form 27 January 2014
Accepted 30 January 2014
Available online 5 February 2014
Editor: G.F. Giudice

ABSTRACT

We consider *ZH* and *WH* production at the Large Hadron Collider, where the Higgs decays to a $b\bar{b}$ pair. We use jet substructure techniques to reconstruct the Higgs boson and construct angular observables involving leptonic decay products of the vector bosons. These efficiently discriminate between the tensor structure of the *HVV* vertex expected in the Standard Model and that arising from possible new physics, as quantified by higher dimensional operators. This can then be used to examine the CP nature of the Higgs as well as CP mixing effects in the *HZZ* and *HWW* vertices separately.

The recently discovered Higgs-like particle [1] at the Large Hadron Collider (LHC) will dominate global particle physics effort for many years to come. Whether or not this is the Standard Model (SM) Higgs boson necessitates precise study of its couplings to other SM particles. Here we focus on the study of the tensor structure and hence of the CP properties of the Higgs-Weak Boson vertex (*HVV*) as well as of CP violating effects in the same, through associated production of a Higgs boson with a $V = W, Z$ boson (*VH* channel). We construct new observables that can be used to disentangle CP even and CP odd new physics contributions from SM contributions (and from each other). Importantly, this channel can probe the *HWW* and *HZZ* vertices *separately*. The *VH* channel, though subdominant, can be studied using modern jet substructure techniques [2]. We show that, interestingly, these techniques automatically enhance the sensitivity of the *VH* channel to probe such anomalous couplings.

The *HVV* vertex can be written as:

$$ig_W M_W \left[A g^{\mu\nu} + B\left(p^\mu q^\nu - g^{\mu\nu} p\cdot q\right) + C\epsilon^{\mu\nu\rho\sigma} p_\rho q_\sigma \right] \qquad (1)$$

where A, B (C) are form factors corresponding to CP even (odd) terms respectively. In the SM $A = 1$ and $B = 0 = C$. We perform a model-independent analysis and show how the *VH* channel can be used to probe such a vertex structure. In the absence, so far, of any signal of physics Beyond the SM (BSM), a precision study of the Higgs is the portal to probe the same. Assuming that this new physics respects SM gauge symmetries, one can characterise it through effective higher dimensional operators. The vertex in Eq. (1) can be generated by supplementing the SM Lagrangian with higher dimensional operators, such as:

$$g_W^2 \frac{c_1}{2\Lambda_1^2} \Phi^\dagger \Phi F_{\mu\nu} F^{\mu\nu}, \qquad g_W^2 \frac{c_2}{2\Lambda_2^2} \Phi^\dagger \Phi \tilde{F}_{\mu\nu} F^{\mu\nu}, \qquad (2)$$

with g_W and $F_{\mu\nu}$ the electroweak coupling constant and SU(2) field strength tensor, $\tilde{F}_{\mu\nu} = \frac{1}{2}\epsilon_{\mu\nu\alpha\beta}F^{\alpha\beta}$, Φ the (SU(2) doublet) Higgs field and c_i (complex) constants. These operators then generate a vertex with $B = 4c_1/\Lambda_1^2$ and $C = 4c_2/\Lambda_2^2$. In the SM the strength of the *HZZ* and *HWW* couplings are related through custodial symmetry. There are however, several extensions of the SM that could modify the coupling strength [3]. In addition BSM physics could also modify the Lorentz structure of the *HVV* vertex as described above. The operators in Eq. (2) are only two of the several possible operators that can contribute to the general *HVV* vertex [4,5]. In principle, the various operators can affect the *HWW* and *HZZ* vertices differently. It, therefore, becomes important to be able to study both the vertices separately to probe signs of new physics in a comprehensive manner. The operators in Eq. (2) are not severely constrained from precision electroweak tests or the electric dipole moment of the electron [6]. Stronger constraints from the decay widths of $H \to V^{(*)}V^*$ and $H \to \gamma\gamma$, may only be extracted after several simplifying assumptions [7,8,6]. Thus, one must *directly* probe the *HVV* vertex in order to arrive at concrete and unambiguous conclusions on the existence of BSM physics. Throughout, for simplicity, we will absorb the coefficients c_1 and c_2 into the scales Λ_1 and Λ_2 respectively. Therefore these do not directly reflect the scale of new physics.

* Corresponding author.

http://dx.doi.org/10.1016/j.physletb.2014.01.069

The *HZZ* interaction in the four lepton channel was investigated in [9,7,10–13] with current LHC data disfavouring a pure pseudoscalar hypothesis at $\sim$2–3σ [14,15]. Similar constraints on the *HWW* vertex using the $H \to W^{(*)}W^*$ decay are hard to achieve since the kinematical cuts necessary to eliminate backgrounds hamper the analysis.

The tensor structure of the *HVV* vertex can be investigated using kinematic and angular correlations [16,17] in Vector Boson Fusion (VBF). However, the Z and W boson contributions cannot be studied separately since the *HZZ* vertex constitutes approximately one-fourth of the total cross-section. Another point to note about VBF is that the momentum-dependent non-SM vertices tend to push the kinematic distribution of the tagging-jets to regions of phase space that are more QCD-like [18]. In order to improve the sensitivity to non-SM couplings the VBF like cuts may need to be relaxed resulting in significant contamination from Higgs production through gluon fusion.

Electron–positron colliders can offer precision information on the *HZZ* vertex [19,20], but an unambiguous separate determination of the *HWW* and *HZZ* vertices through VBF is possible only at the proposed LHeC [21]. Hence, in order to elucidate the nature of the *HVV* couplings at the LHC, one is unavoidably led to *VH* production.

At the LHC, where until recently even the detection of the Higgs in the *VH* channel was considered difficult, studies of the nature of the *HVV* vertex, in the same, were not contemplated. Here we show that modern jet substructure techniques [2], of use when the Higgs is highly boosted and decays to a $b\bar{b}$ pair, can not only probe but also increase the sensitivity to BSM couplings. We furthermore demonstrate that angular correlations of decay leptons produced in the *VH* process, are able to determine the vertex in Eq. (1). We simulate all processes using `MadGraph5` [22] interfaced with `Pythia6` [23] for showering and hadronisation, and use the `FastJet` package [24] to cluster the jets. The effective Lagrangian was implemented in `FeynRules` [25].

1. Event selection

It is important to apply selection criteria to distinguish between the signal and background processes. For *ZH* production we require:

1. A fat jet (radius $R = 1.2$, $p_T > 200$ GeV). After applying the mass drop and filtering procedure of [2], we require no more than three subjets with $p_T > 20$ GeV, $|\eta| < 2.5$, and radius $R_{sub} = \min(0.3, R_{bb})$, where R_{bb} is the separation of the two hardest subjets, both of which must be b-tagged. We also require that the invariant mass of this jet system reconstructs the Higgs mass in the range 115–135 GeV.
2. Exactly 2 leptons (transverse momentum $p_T > 20$ GeV, pseudorapidity $|\eta| < 2.5$) of same flavour and opposite charge, with invariant mass within 10 GeV of the Z mass M_Z. These should be isolated: the sum of all particle transverse momenta in a cone of radius $R = 0.3$ about each lepton should not exceed 10% of that of the lepton.
3. Demand that the reconstructed Z has a $p_T > 150$ GeV, with azimuthal angle satisfying $\Delta\phi(Z, H) > 1.2$.

After cuts, the only significant surviving background process is Z + jets. Cross-sections at Leading Order (LO) after cuts are shown in Table 1. The $H \to b\bar{b}$ branching ratios were taken from Ref. [26]. Since the K factors for the background and the signal are not too different [2] our results are not expected to be significantly different at Next to Leading Order (NLO). In principle our analysis is sensitive to the b-tagging efficiency and light quark jet rejection rate [2] (here set to $\epsilon_b = 0.6$ and $r_j = 100$ respectively). However, we checked that this has no impact on the angular observables. Note that the V + jets backgrounds were evaluated with up to three extra partons in the 5 flavour scheme, i.e. including the dominant $Vb\bar{b}$ background.

Table 1
Cross-sections (fb) evaluated at leading order for the 14 TeV LHC after applying all cuts. V + jets corresponds to the Z + jets background for the *ZH* process and W + jets for the *WH* process. For the last two columns the SM contribution was set to zero and the values of Λ_i were set to reproduce the SM total cross-section before applying cuts. These results do not require W reconstruction.

Channel	$VH_{\rm SM}$	V + jets	$t\bar{t}$	Single top	$VH^{0^+}_{\rm BSM}$	$VH^{0^-}_{\rm BSM}$
ZH	0.12	0.23	0	0	0.48	0.73
WH	0.355	0.28	0.13	0.06	1.45	2.14

For *WH* production we require:

1. The Higgs reconstructed as above.
2. Exactly 1 hard lepton ($p_T > 30$ GeV, $|\eta| < 2.5$), isolated as above.
3. Missing transverse momentum $\not{p}_T > 30$ GeV.
4. The reconstructed W has $p_T > 150$ GeV and azimuthal angle satisfying $\Delta\phi(H, W) > 1.2$.
5. No additional jet activity with $p_T^{jet} > 30$ GeV, $|\eta| < 3$ (to suppress single and top pair production backgrounds).

Again, major backgrounds are detailed in Table 1.

1.1. Reconstructing the neutrino momentum

One must reconstruct the neutrino in *WH* production to determine our angular observables. We identify the neutrino transverse momentum $\vec{p}_{T\nu}$ with the missing transverse momentum $\vec{\not{p}}_T$. The missing transverse momentum is approximated by taking the negative vector sum of the transverse momentum of all particles that can be detected (>0.5 GeV). In order to evaluate the full four momentum of the neutrino, we demand that the squared sum of the neutrino and lepton momenta be equal to the squared W boson mass ($(p_\nu + p_{l_1})^2 = M_W^2$), solving the resulting quadratic equation. Comparing with the "true" Monte-Carlo generated neutrino momentum, we find that choosing a given solution out of the two possible ones, reconstructs the true neutrino momentum 50% of the time, with $\simeq$5% giving imaginary solutions. One can also compare the boosts of the Higgs β_z^H and reconstructed W β_z^W in the z direction. The solution with the minimum value for $|\beta_z^W - \beta_z^H|$ gives the true neutrino momentum in 65% of cases. We present all our results using the latter algorithm.

1.2. Sensitivity to new operators

The BSM operators of Eq. (2) push the p_T, invariant mass ($\sqrt{\hat{s}_{HV}}$) and rapidity separation (Δy_{HV}) distributions of the *VH* system to larger values [18,27,28], leading to larger Higgs boosts and a reduced separation between the leptons (R_{ll}), and b jets R_{bb}. Consequently, the above selection cuts enhance BSM effects. In Table 1, one sees the acceptance of these operators to the selection cuts is very good: $\sim$4 ($\sim$6) times the SM acceptance for the CP even (odd) operator.

In Fig. 1, we consider the SM Lagrangian supplemented by either the CP odd or even operator applied to the *WH* channel. We show the ratio of the SM + BSM and SM cross-sections both for the total cross-section ($R^{\pm}_{tot} = \sigma^{\rm SM+BSM\pm}_{tot}/\sigma^{\rm SM}_{tot}$) and the cross-section after applying selection cuts ($R_{jetsub}\pm = \sigma^{\rm SM+BSM\pm}_{jetsub}/\sigma^{\rm SM}_{jetsub}$). As expected, the BSM contribution is larger for smaller values of the

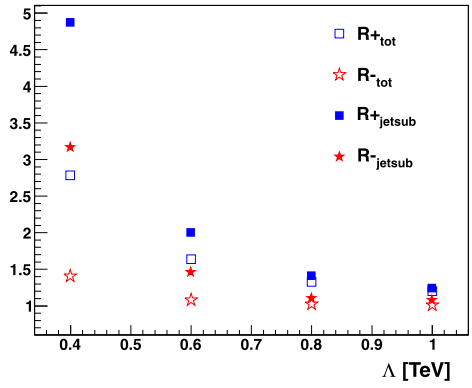

Fig. 1. The ratio of the cross-sections $R-$ (mixture of SM and CP odd) (red stars) and $R+$ (mixture of SM and the BSM CP even term) (blue boxes) both before (hollow markers) and after (bold markers) applying selection cuts for the WH channel. The scale of new physics Λ determines the strength of the contribution from new physics.

new physics scales Λ_i. We also see that R_{jetsub} increases at a faster rate than R_{tot} with decreasing values of Λ_i. While the rates alone cannot provide information about the HVV interactions, the variation of the rates with the p_T cuts used can provide information on the presence of BSM physics. This behaviour would also be observable in both $pp \to ZH \to l\bar{l}b\bar{b}$ and $pp \to ZH \to \nu\bar{\nu}b\bar{b}$.

2. Angular observables

To fully distinguish CP even and odd BSM contributions, one must construct CP-odd observables, which is difficult in principle [29]. For ZH production, Ref. [30] considered two such observables, although these are sensitive to radiation and hadronisation corrections; Ref. [31] defined observables which are insensitive to the CP nature of BSM contributions. Ref. [32] examined WH production with the decay $H \to W^{(*)}W^*$, though the effect of the BSM CP even term was not considered. Although the transverse mass of the VH system has been used at the Tevatron to probe the HWW vertex [33] it has been shown to be ineffective at the LHC [27]. However, the Lorentz structure of the BSM vertices will be reflected in the angular distribution of the gauge boson's decay products. The momenta of the V and Higgs bosons are reconstructed from the leptons and jets as follows:

$$p_V = p_{l_1} + p_{l_2}, \qquad p_H = p_{b_1} + p_{b_2} + p_j, \tag{3}$$

where $\{p_{b_i}\}$ are the momenta of the b jets, p_j is the momentum of the light quark jet if it is reconstructed and p_{l_1} and p_{l_2} are the momenta of the lepton and the anti-lepton respectively (for WH, p_{l_1} corresponds to the lepton momentum and p_{l_2} to the neutrino). With these momenta, we may define

$$\cos\theta^* = \frac{\vec{p}_{l_1}^{(V)} \cdot \vec{p}_V}{|\vec{p}_{l_1}^{(V)}||\vec{p}_V|}, \qquad \cos\delta^+ = \frac{\vec{p}_{l_1}^{(V)} \cdot (\vec{p}_V \times \vec{p}_H)}{|\vec{p}_{l_1}^{(V)}||\vec{p}_V \times \vec{p}_H|},$$
$$\cos\delta^- = \frac{(\vec{p}_{l_1}^{(H-)} \times \vec{p}_{l_2}^{(H-)}) \cdot \vec{p}_V}{|(\vec{p}_{l_1}^{(H-)} \times \vec{p}_{l_2}^{(H-)})||\vec{p}_V|}. \tag{4}$$

Here $\vec{p}_X^{(Y)}$ corresponds to the three momentum of the particle X in the rest frame of the particle Y. If Y is not specified then the momentum is defined in the lab frame. Momenta labels are as follows: H corresponds to the Higgs boson, $H-$ stands for the four momentum obtained when the sign of the spatial component of the Higgs momentum is inverted ($\vec{p}_H \to -\vec{p}_H$) and $V = W^{\pm}, Z$. For example, $\vec{p}_{l_1}^{(H-)}$ refers to the lepton's momentum after boosting to a frame in which the Higgs would be at rest, were its momentum reversed.

The angle $\cos\theta^*$, first defined in [19], encodes the W boson polarisation. The SM and BSM couplings lead to mostly longitudinal or transverse W bosons respectively. That $\cos\theta^*$ then effectively distinguishes SM and BSM effects can be seen in Fig. 2, which also includes the $W+$jets background. To distinguish the two BSM contributions, one needs different observables, namely $\cos\delta^{\pm}$, also shown in Fig. 2. Results for ZH production (not shown) are qualitatively similar.

2.1. Asymmetries

Motivated by Fig. 2, we define asymmetry parameters

$$A(X) = \frac{\sigma(|X| < 0.5) - \sigma(|X| > 0.5)}{\sigma(|X| < 0.5) + \sigma(|X| > 0.5)} \tag{5}$$

pure BSM and the dominant background are shown for ZH and WH production in Tables 2 and 3 respectively. We see that $A(\cos\theta^*)$ discriminates SM from pure BSM contributions for both WH and ZH production. The other angles discriminate the BSM CP odd and even vertices. We have checked that in WH production, reconstruction ambiguities of the W shift the absolute value of the asymmetries by roughly the same amount and thus differences in asymmetries are robust against this systematic uncertainty.

Fig. 3 shows the Λ_i dependence of these asymmetries in WH production, including BSM and SM operators. We set $A = 1$ and vary B and C in turn, whilst including the dominant Wjj background. As expected, the asymmetries approach the SM value with

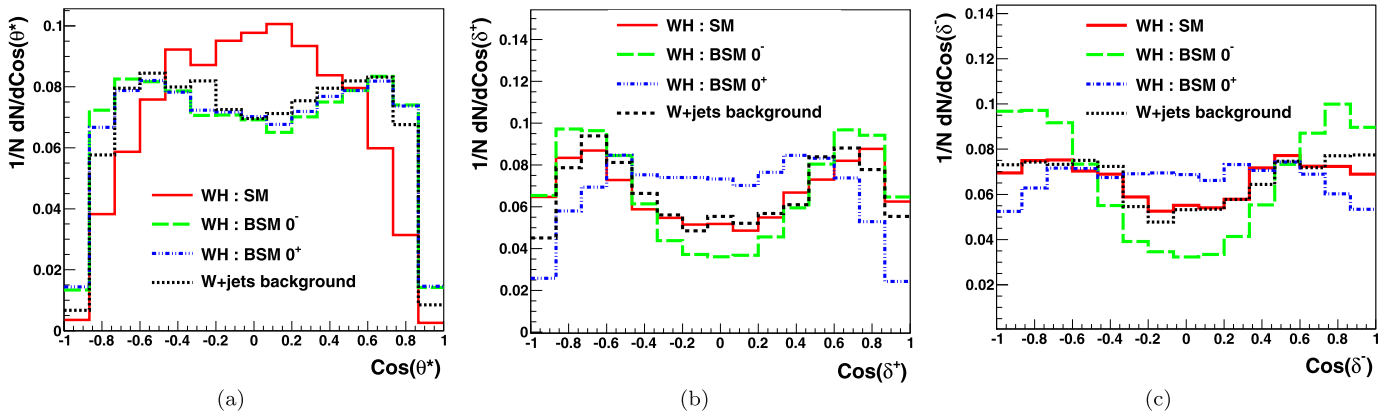

(a) (b) (c)

Fig. 2. Distributions of the angles defined in Eq. (4) for WH production in the SM (solid red lines), pure BSM CP even (dot-dashed blue lines), pure BSM CP odd (dashed green lines) and for the dominant $W+$jets background (dotted black lines). (a) $\cos\theta^*$, (b) $\cos\delta^+$, (c) $\cos\delta^-$.

Table 2
Asymmetries for the angles defined Eq. (4) in ZH production for the SM and BSM vertices at 14 TeV LHC after application of all cuts.

Asymmetries	$ZH_{\rm SM}$	$ZH^{0-}_{\rm BSM}$	$ZH^{0+}_{\rm BSM}$	$Z+$jets
$A(\cos\theta^*)$	0.35	−0.05	−0.02	0.07
$A(\cos\delta^+)$	−0.207	−0.262	0.088	−0.188
$A(\cos\delta^-)$	−0.209	−0.435	−0.103	−0.321

Table 3
Asymmetries for the angles defined Eq. (4) in WH production for the SM and BSM vertices at 14 TeV LHC after application of all cuts.

Asymmetries	$WH_{\rm SM}$	$WH^{0-}_{\rm BSM}$	$WH^{0+}_{\rm BSM}$	$W+$jets
$A(\cos\theta^*)$	0.396	0.073	0.100	0.142
$A(\cos\delta^+)$	−0.150	−0.284	0.142	−0.138
$A(\cos\delta^-)$	−0.058	−0.353	0.042	−0.118

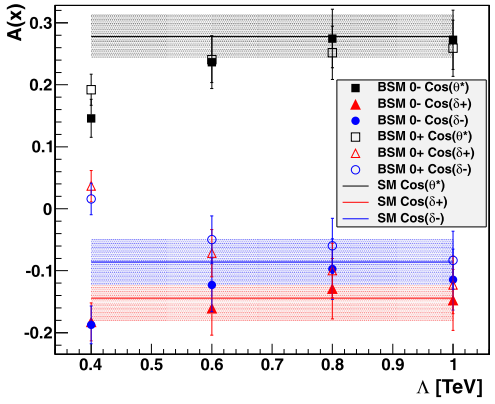

Fig. 3. The value of the asymmetries defined in Eq. (5) The strength of the BSM contribution is varied through the parameters Λ_i. The horizontal lines indicate the asymmetry in the SM. The contribution from the dominant Wjj background is included in the evaluation of these asymmetries. The 1σ statistical uncertainty in the determination of these asymmetries for 300 fb^{-1} of data for 14 TeV LHC is shown by the shaded regions for SM and by the error bars for BSM scenarios.

increasing Λ_i. For $\cos\theta^*$ both BSM operators reduce the asymmetry; for $\cos\delta^\pm$ their effects are of opposite sign, allowing to effectively discriminate the BSM contributions. Similar results are obtained for ZH production, and Fig. 3 also includes estimated statistical uncertainty. Bounds of $\Lambda_i > 400$ GeV can be easily placed with 300 fb^{-1} of LHC data. Obviously the suggested reach of 3000 fb^{-1} of data for LHC will reduce the uncertainties and allow larger p_T cuts to improve the sensitivity to BSM couplings. In comparison with Higgs decay rates, we note that an unambiguous determination of each of the terms is hard to achieve although some bounds can be placed: e.g. Ref. [6] suggests that $\Lambda_1 > 250$ GeV may still be allowed for the CP even BSM coupling. Similar bounds are expected for the CP odd couplings.[1]

3. Conclusions

We examine ZH and WH production at the LHC, where the Higgs decays to a $b\bar{b}$ pair. Combining jet substructure techniques with vector boson polarisation (via angular distributions of decay products), we give observables that can distinguish between new operators coupling the Higgs to vector bosons. Importantly (given that the newly discovered boson cannot be purely CP-odd), our analysis applies when both BSM and SM operators are present, and mutually interfere. We show that in VH production, sensitivity to BSM physics is enhanced through an increased acceptance of BSM couplings to the selection cuts, and the HWW and HZZ couplings can be studied independently of each other. This increased acceptance means that with higher luminosity and energy, one can afford larger values of the transverse momentum cut and thus enhance the sensitivity of this channel to BSM physics. In fact, as can be seen from Fig. 3, even the study of a *single* asymmetry can provide 2σ bounds on $\Lambda_i \sim 400$ GeV, which reduces to 1σ for $\Lambda_i = 600$ GeV, for 300 fb^{-1} of data at the 14 TeV LHC. With a luminosity of 3000 fb^{-1}, 2σ bounds on $\Lambda_i = 600$ GeV are easily achieved. It is clear that combining the asymmetries and/or a multivariate analysis, can only add to this sensitivity. Further investigations, including possible detector effects, are in progress.

[1] Under some highly restrictive assumptions one can restrict $\Lambda_2 > 900$ GeV using Higgs decay rates [34].

Acknowledgements

We thank D. Sengupta for discussions regarding W reconstruction and S. Vempati for comments on the manuscript. KM acknowledges the financial support from CSIR India, the French CMIRA and ENIGMASS Labex. DJM and CDW thank the Indian Institute of Science for their hospitality while part of this work was carried out. DJM acknowledges partial support from the Royal Society of Edinburgh, the Indian National Science Academy and the STFC. RG wishes to thank the Department of Science and Technology, Government of India, for support under grant no. SR/S2/JCB-64/2007.

References

[1] S. Chatrchyan, et al., CMS Collaboration, Phys. Lett. B 716 (2012) 30, arXiv:1207.7235 [hep-ex];
G. Aad, et al., ATLAS Collaboration, Phys. Lett. B 716 (2012) 1, arXiv:1207.7214 [hep-ex].
[2] J.M. Butterworth, A.R. Davison, M. Rubin, G.P. Salam, Phys. Rev. Lett. 100 (2008) 242001, arXiv:0802.2470 [hep-ph];
M.H. Seymour, Z. Phys. C 62 (1994) 127.
[3] M. Farina, C. Grojean, E. Salvioni, J. High Energy Phys. 1207 (2012) 012, arXiv:1205.0011 [hep-ph];
S. Kanemura, M. Kikuchi, K. Yagyu, Phys. Rev. D 88 (2013) 015020, arXiv:1301.7303 [hep-ph];
J. Diaz-Cruz, D. Lopez-Falcon, Phys. Lett. B 568 (2003) 245, arXiv:hep-ph/0304212.
[4] W. Buchmuller, D. Wyler, Nucl. Phys. B 268 (1986) 621.
[5] R. Contino, M. Ghezzi, C. Grojean, M. Muhlleitner, M. Spira, J. High Energy Phys. 1307 (2013) 035, arXiv:1303.3876 [hep-ph];
B. Grzadkowski, M. Iskrzynski, M. Misiak, J. Rosiek, J. High Energy Phys. 1010 (2010) 085, arXiv:1008.4884 [hep-ph].
[6] E. Masso, V. Sanz, Phys. Rev. D 87 (2013) 033001, arXiv:1211.1320 [hep-ph];
D. McKeen, M. Pospelov, A. Ritz, Phys. Rev. D 86 (2012) 113004, arXiv:1208.4597 [hep-ph].
[7] R.M. Godbole, D. Miller, M.M. Muhlleitner, J. High Energy Phys. 0712 (2007) 031, arXiv:0708.0458 [hep-ph].
[8] K. Hagiwara, R. Szalapski, D. Zeppenfeld, Phys. Lett. B 318 (1993) 155, arXiv:hep-ph/9308347.
[9] S. Choi, D. Miller, M. Muhlleitner, P. Zerwas, Phys. Lett. B 553 (2003) 61, arXiv:hep-ph/0210077.
[10] Y. Gao, A.V. Gritsan, Z. Guo, K. Melnikov, M. Schulze, et al., Phys. Rev. D 81 (2010) 075022, arXiv:1001.3396 [hep-ph].
[11] A. De Rujula, J. Lykken, M. Pierini, C. Rogan, M. Spiropulu, Phys. Rev. D 82 (2010) 013003, arXiv:1001.5300 [hep-ph].
[12] S. Bolognesi, Y. Gao, A.V. Gritsan, K. Melnikov, M. Schulze, et al., Phys. Rev. D 86 (2012) 095031, arXiv:1208.4018 [hep-ph].
[13] D. Stolarski, R. Vega-Morales, Phys. Rev. D 86 (2012) 117504, arXiv:1208.4840 [hep-ph].
[14] Measurements of the properties of the Higgs-like boson in the four lepton decay channel with the ATLAS detector using 25 fb^{-1} of proton–proton collision data, Tech. Rep. ATLAS-CONF-2013-013, CERN, Geneva, 2013;
Properties of the Higgs-like boson in the decay H to ZZ to 4l in pp collisions at sqrt s =7 and 8 TeV, Tech. Rep. CMS-PAS-HIG-13-002, CERN, Geneva, 2013.
[15] S. Chatrchyan, et al., CMS Collaboration, Phys. Rev. Lett. 110 (2013) 081803, arXiv:1212.6639 [hep-ex].
[16] T. Plehn, D.L. Rainwater, D. Zeppenfeld, Phys. Rev. Lett. 88 (2002) 051801, arXiv:hep-ph/0105325.

[17] V. Hankele, G. Klamke, D. Zeppenfeld, T. Figy, Phys. Rev. D 74 (2006) 095001, arXiv:hep-ph/0609075.
[18] A. Djouadi, R. Godbole, B. Mellado, K. Mohan, arXiv:1301.4965 [hep-ph], 2013.
[19] D. Miller, S. Choi, B. Eberle, M. Muhlleitner, P. Zerwas, Phys. Lett. B 505 (2001) 149, arXiv:hep-ph/0102023;
T. Han, J. Jiang, Phys. Rev. D 63 (2001) 096007, arXiv:hep-ph/0011271;
S.D. Rindani, P. Sharma, Phys. Rev. D 79 (2009) 075007, arXiv:0901.2821 [hep-ph].
[20] S.S. Biswal, D. Choudhury, R.M. Godbole, Mamta, Phys. Rev. D 79 (2009) 035012, arXiv:0809.0202 [hep-ph];
S.S. Biswal, R.M. Godbole, Phys. Lett. B 680 (2009) 81, arXiv:0906.5471 [hep-ph];
S. Dutta, K. Hagiwara, Y. Matsumoto, Phys. Rev. D 78 (2008) 115016, arXiv:0808.0477 [hep-ph].
[21] S.S. Biswal, R.M. Godbole, B. Mellado, S. Raychaudhuri, Phys. Rev. Lett. 109 (2012) 261801, arXiv:1203.6285 [hep-ph].
[22] J. Alwall, M. Herquet, F. Maltoni, O. Mattelaer, T. Stelzer, J. High Energy Phys. 1106 (2011) 128, arXiv:1106.0522 [hep-ph].
[23] T. Sjostrand, S. Mrenna, P.Z. Skands, J. High Energy Phys. 0605 (2006) 026, arXiv:hep-ph/0603175.
[24] M. Cacciari, G.P. Salam, G. Soyez, Eur. Phys. J. C 72 (2012) 1896, arXiv:1111.6097 [hep-ph].
[25] N.D. Christensen, C. Duhr, Comput. Phys. Commun. 180 (2009) 1614, arXiv:0806.4194 [hep-ph].
[26] LHC Higgs Cross Section Working Group, S. Dittmaier, C. Mariotti, G. Passarino, R. Tanaka (Eds.), CERN-2011-002, CERN, Geneva, 2011, arXiv:1101.0593 [hep-ph].
[27] J. Ellis, D.S. Hwang, V. Sanz, T. You, J. High Energy Phys. 1211 (2012) 134, arXiv:1208.6002 [hep-ph].
[28] C. Englert, M. Spannowsky, M. Takeuchi, J. High Energy Phys. 1206 (2012) 108, arXiv:1203.5788 [hep-ph].
[29] T. Han, Y. Li, Phys. Lett. B 683 (2010) 278, arXiv:0911.2933 [hep-ph].
[30] N.D. Christensen, T. Han, Y. Li, Phys. Lett. B 693 (2010) 28, arXiv:1005.5393 [hep-ph].
[31] C. Englert, D. Goncalves-Netto, K. Mawatari, T. Plehn, J. High Energy Phys. 1301 (2013) 148, arXiv:1212.0843 [hep-ph].
[32] N. Desai, D.K. Ghosh, B. Mukhopadhyaya, Phys. Rev. D 83 (2011) 113004, arXiv:1104.3327 [hep-ph].
[33] E. Johnson, arXiv:1305.3675 [hep-ex], 2013.
[34] K. Cheung, J.S. Lee, P.-Y. Tseng, J. High Energy Phys. 1305 (2013) 134, arXiv:1302.3794 [hep-ph].